

## Fully Automatic Segmentation Method of Pathological Periventricular White Matter Changes Using Morphological Features

Ik-Hwan Cho<sup>1</sup>, In-Chan Song<sup>2</sup>, Jung-Su Oh<sup>3</sup>, Dong-Seok Jeong<sup>1</sup>

<sup>1</sup> Department of Electronic Engineering, College of Engineering, Inha University

<sup>2</sup> Department of Radiology, Seoul National University Hospital

<sup>3</sup> Interdisciplinary Program of Biomedical Engineering, Seoul National University

(Received September 1, 2005. Accepted November 21, 2005)

**Abstract:** Age-related White Matter Changes (WMC) on Magnetic Resonance Imaging (MRI) are known to appear frequently in Multiple sclerosis (MS) and Alzheimer's disease and to be related to cognitive impairment. The characterization of these WMC is very important to the study of psychology and aging. These changes consist of periventricular and subcortical types, however it is difficult to detect and segment WMC using only intensity-based methods, because their intensity level is similar to that of the gray matter (GM). In this paper, we propose a new method of segmenting periventricular WMC using K-means clustering and morphological features.

**Key words:** White matter change, K-means clustering, Skull and scalp stripping, Segmentation, Region growing, Morphology

### INTRODUCTION

White matter changes (WMC) or white matter lesions frequently appear in elderly subjects with age-related pathologies [1]. In general, pathologies such as MS and Alzheimer's disease are known to induce these WMC, which are thought to be related to cognitive impairment [2], [3], [4], [5], [6]. Quantitative characterization of the detected WMC is essential for the assessment of disease progression and treatment efficacy.

MRI is one of the most useful methods of detecting and segmenting WMC. In general, studies based on MRI have used several types of images, such as T2-weighted, Proton Density (PD)-weighted, T1-weighted and Fluid Attenuated Inversion Recovery (FLAIR) images. WMC usually exhibit high intensity in both PD-weighted and T2-weighted images, while they appear as regions of low intensity in T1-weighted images. To detect and segment these WMC correctly, it is important to properly utilize the relation between them. T2-weighted and PD-weighted images are usually used together, because they involve a short

scan time relative to any other sequences.

Most previous methods used manual or semi-automatic schemes to segment WMC correctly [7], [8]. Segmentation is performed by experts who are well trained medical specialists not physicians or engineering staffs. Therefore its results have very low possibility to be false. Pannizo et al. first used a supervised automatic procedure to discriminate between the brain tissue, fat and the skull, and then went on to develop an algorithm based on a histogram analysis that detects white matter lesions, such as those associated with MS [9]. Some of the previously developed WMC detection methods including brain tissue segmentation have used intensity-based clustering schemes, based on the fact that each type of tissue has a different intensity level [10], [11]. K-means clustering is basic scheme to be used for usual segmentation including general image application [12]. Warfield proposed an algorithm to segment multichannel brain image using K-NN(Nearest Neighbors) classification rule [10]. Mohamed et al. used a modified fuzzy c-means clustering method to segment brain tissues in CT and MR [11]. The method in [11] is inspired from Markov Random Field (MRF) and robust against noise by modifying the conventional fuzzy c-means algorithm. Ardizzone et al. also utilized the modified fuzzy c-means method to detect MS in MR images [13]. They used new two channel fuzzy c-means model since both T2 and PD images were used. Recently statistical algorithms are widely used to

---

**Corresponding Author :** In-Chan Song  
Department of Radiology, Seoul National University Hospital,  
28 Yongon-Dong, Chongno-Gu, Seoul, Korea  
Tel. 02-2072-3941, Fax. 02-763-0379  
E-mail. icsong@radcom.snu.ac.kr

discriminate brain tissues precisely. Expectation maximization-based method proposed by Joshi et al. fits compartment statistics of brain structure into sub tissue voxels [14].

Classical manual segmentation method relies on the observer's subjective decision. Because of the observer's subjectivity, however, this method has observer variability. In an attempt to decrease this high observer variability, basic segmentation algorithms, such as thresholding strategies [15], region growing [16], were frequently employed with manual interaction. However, even though manual schemes can produce good results for individual cases, their reproducibility cannot be guaranteed and, therefore, the results obtained from manual schemes are difficult to be analyzed statistically and used as objective measures, because of their limited reliability. In addition, manual analyses of a large number of MR images performed by human experts are extremely time consuming processes. Therefore, there is a pressing need for an automated method of segmenting white matter lesions that can analyze a large amount of image data in a reproducible way. For intensity-based clustering schemes, they often produce incorrect results, since the intensity level of the WMC is similar to that of other tissue, and because of the existence of intensity variability, such as RF inhomogeneity [17] and partial volume effects [18]. Therefore, the ambiguous discrimination between normal tissue and lesions may cause the decrease of reliability of the segmentation process. Some methods may use an iterative user interaction, in order to handle problems such as noise and RF inhomogeneity [17]. In addition, although statistical method is very logical and represents good results, but they may also require some manual interaction as algorithm of needs some manual segmentation by expert to resolve partial gray-white voxel problem [14].

In this paper, we propose a new scheme to correctly detect and segment WMC using intensity-based clustering and morphological features. Since this research range is limited to periventricular WMC except sub-cortical WMC, material and methods are chosen according to it. Moreover, based on various experiments, we showed that the proposed method provides an effective means of segmenting WMC.

## MATERIAL

The proposed method was implemented using IDL (Interactive Data Language, Research Systems, Inc) on a Pentium 4 1.6GHz PC. MR imaging was performed with a 1.5-T unit (Magnetom Vision Plus, Siemens, Germany) using a quadrature transmit/receive head coil. Contiguous transverse dual FSE PD-weighted and T2-weighted images were obtained with 3400/18/90 (TR/TE/effective TE), 3-mm-thick sections (contiguous and interleaved), 22x22cm FOV, a 256 x 192 matrix

size, >50 sections, an echo train length of eight, and a 0.86-mm pixel size. Our experiments used T2-weighted and PD-weighted axial images of Alzheimer's disease patients and some normal subjects. Each image set had 40~45 slices and covered the whole brain. Because the proposed method focused on the segmentation and detection of the periventricular WMC, which are adjacent to the lateral ventricle, we restricted the target images to slices which included the lateral ventricle. However, the development of an automatic detection algorithm for slices which include the lateral ventricle in 3D image data may represent an altogether different problem and, therefore, this issue was not covered in this paper. In this study, we heuristically decided the target slices to use for the experiments. We experiment with several patient's data and Fig. 9 and Fig. 10 shows overall process of the proposed method and Table 1 represents final detection results for others.

## METHODS

### Overall Scheme and MR Imaging

Fig. 1 shows the entire block diagram of the proposed method used to detect and segment the WMC correctly. Firstly, non-brain regions such as the skull, fat and face muscle are removed from the PD images using the multi-seeds region growing method based on our brain model which uses prior knowledge about the shape of the brain. The proposed skull and scalp stripping is very important step since its result may affect the consecutive processes. Then, the intracranial brain mask image obtained from the PD image is applied to the T2 image. Secondly, the cerebrospinal fluid (CSF) is segmented automatically using the ratio image of the PD image to the T2 image [19], [20] and the Ostu thresholding method [15]. Thirdly, the GM and white matter (WM) are segmented in the PD image using the K-means clustering method [12]. Finally, the periventricular WMC are detected using morphological features, which is that the WMC are adjacent to the lateral ventricle and have an intensity level similar to GM.

### The Skull and Scalp Stripping Process

Before the segmentation of the CSF, GM and WM, however, it is necessary to remove any non-brain regions. We use a hybrid method, involving an application of the region growing method to the T2-weighted and PD-weighted images, in order to remove the skull [16]. To use this hybrid method with the T2-weighted and PD-weighted images, both images must be scanned in the same slice position. To remove the skull, initial seed points for region growing are selected. To select appropriate initial seed points, a rectangle

was drawn around the brain and four initial points were obtained using our brain localization model. Fig. 2 shows the brain localization model used for the skull and scalp stripping process.

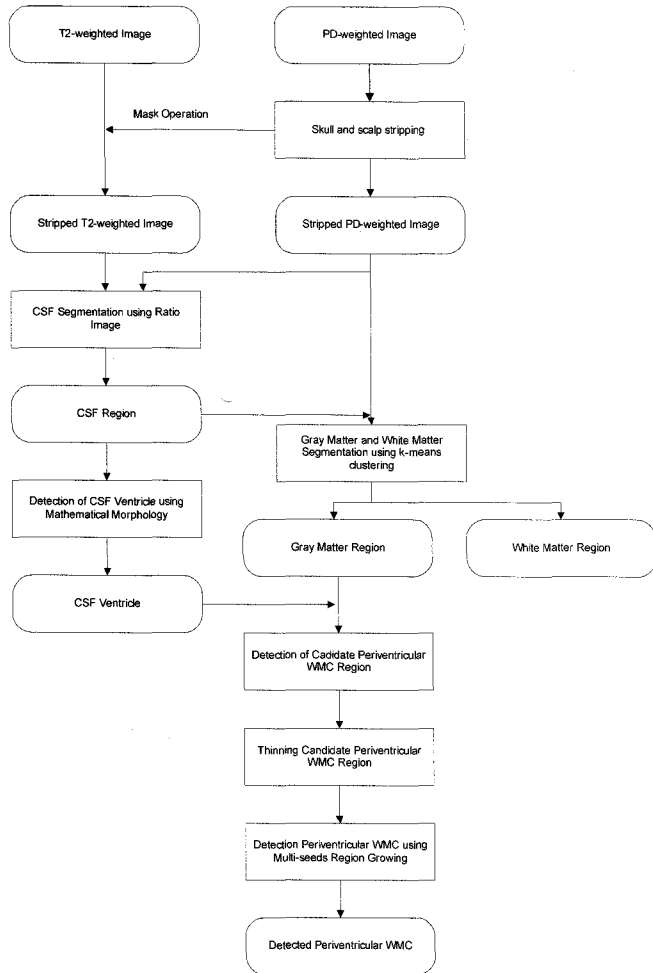


Fig. 1. Overall block diagram of the proposed method.

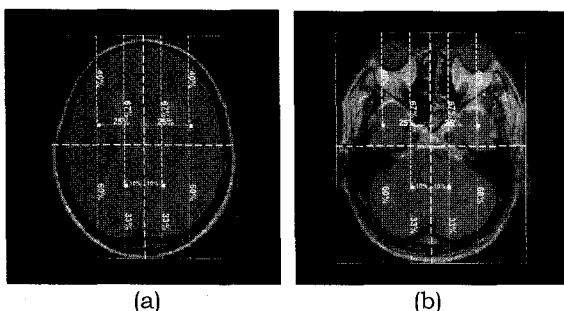


Fig. 2. The proposed brain localization model for the (a) cerebrum and (b) cerebellum. Four white points are used as the initial seed points of the region growing method.

Our model is designed to represent the location of the brain material excluding any non-brain regions and to help select the initial seed points. The locations of the seed points are considered for the distribution of the brain material in the cerebellum rather than in the cerebrum. If the target is limited to the cerebrum, the selection of just two points in the front lobe or parietal lobe is sufficient. Fig. 3 shows the process used to draw the rectangle surrounding the brain and the selection of the four initial points.

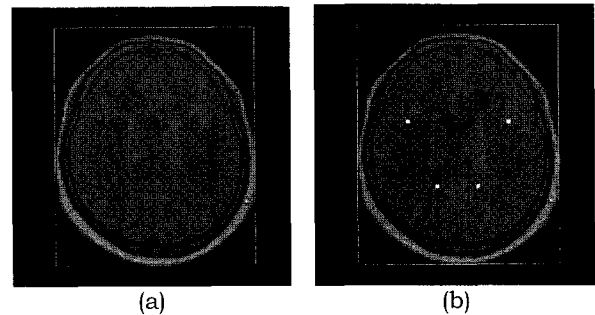


Fig. 3. (a) Rectangle to surround brain skull, (b) Selection of four initial points for region growing.

After the selection of the initial points in the PD-weighted images, the region growing method is independently applied starting from each initial point, because the brain parenchyma is divided into several parts [16]. The four segmented masks obtained by the previous region growing method are merged together and, then, the brain parenchyma mask is obtained in the PD-weighted image. To obtain the stripped images from the T2-weighted image, the brain parenchyma mask obtained from the PD-weighted image is applied to the T2-weighted image. This is possible because the T2- and PD-weighted images are scanned in just equal slice positions. Fig. 4 shows the resultant images obtained from the above operations.

### CSF Segmentation in T2- and PD-weighted Images

After obtaining the stripped brain images, the CSF, GM and WM are segmented sequentially. MRI is a parameter-specific imaging method and, therefore, each specific imaging method provides high contrast or high intensity discrimination for specific tissues. T2-weighted images show high intensity for the CSF parts, while PD-weighted images show high contrast between the GM and WM. Therefore, the different characteristics of each imaging sequence can be used

in tissue segmentation. In this study, however, in order to segment the CSF region, we used the ratio image of the PD-weighted image to the T2-weighted image [18], [19], based on Equation (1) and the Ostu thresholding method [15].

$$\text{Ratio Image} = \frac{PD}{T2} \quad (1)$$

In the ratio image, the CSF region appears darker than any other region, including the GM and WM and, therefore, it can be segmented by clustering the light and dark parts using the Ostu thresholding method (Fig. 5).

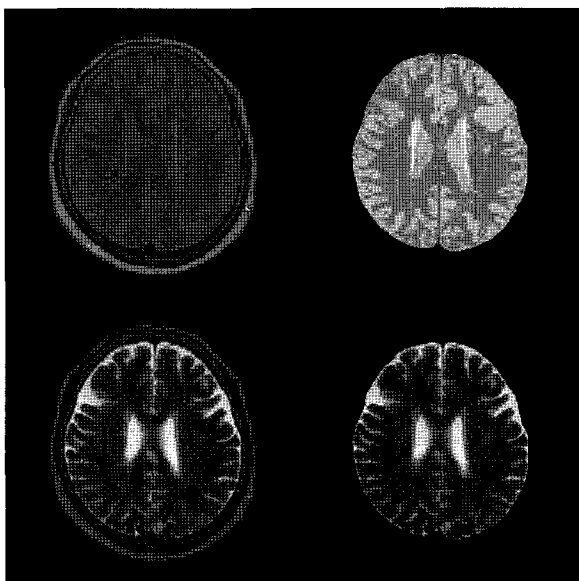


**Fig. 4.** The stripped images using the multi-seeds region growing method and the mask operation. The top two images represent the original PD-weighted image and its stripped version, respectively. The bottom two images represent the original T2-weighted image and its stripped version, respectively.

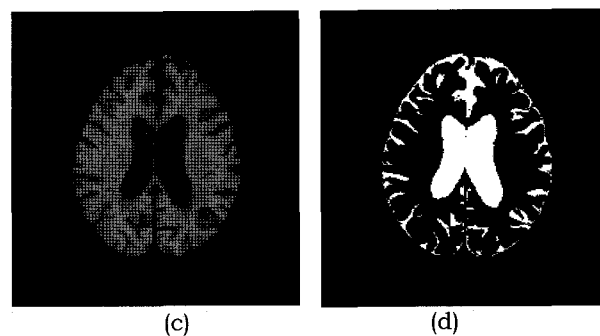
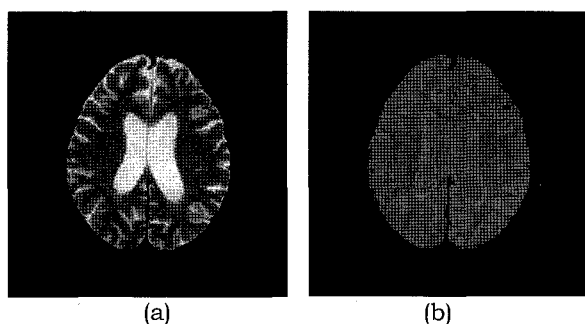


**Fig. 5.** CSF segmentation process. (a) Stripped T2-weighted image, (b) stripped PD-weighted image, (c) ratio image of PD-weighted image to T2-weighted image, (d) segmented CSF region using the Ostu thresholding method.

#### GM and WM Segmentation in PD-weighted Image

In order to segment the GM and WM, the K-means clustering method is used [12]. Because the PD-weighted image has high contrast between the GM and WM, as mentioned in the above section, the intensity-based clustering method can be used to segment the GM and WM. Firstly, we subtract the CSF region obtained from the stripped PD-weighted image described in the previous section. Then, the K-means clustering method is applied to the subtracted images, in order to segment the GM and WM. The GM and WM regions are obtained by clustering with a specific number of clusters, merging some regions and then merging the remaining regions. In this paper, the number of clusters used for the GM-WM segmentation in the PD-weighted images was set to four, because of the partial volume effect. The GM mask is the highest level region and the WM mask is obtained by merging the second and third level regions, while the lowest level represents the background. Fig. 6 shows the result of the segmentation process for the GM and WM.

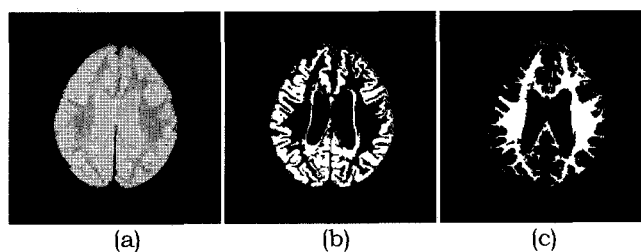


**Fig. 6.** GM and WM segmentation process. (a) Stripped PD-weighted image, (b) segmented GM region and (c) segmented WM region.

### Detection of Lateral Ventricle in Segmented CSF Image and Segmentation of Periventricular WMC

In this method, firstly, the lateral ventricle must be detected, in order to segment the periventricular WMC using the relation between the lateral ventricle and the WMC. In the CSF mask of Fig. 7(a), the lateral ventricle appears as a set of a few large blobs of simple shape, while the subarachnoid space appears in the form of a thin continuous material. Therefore, the lateral ventricle can be accurately detected using the difference between the shapes of these two regions. Because the CSF regions were detected in the previous step, the separation between the lateral ventricle and the subarachnoid space can be readily accomplished. In this study, 2D mathematical morphology [21] and region labeling methods were used. In this study, we used the opening method, which is defined as follows:

$$\text{Opening: } A \circ B = (A \square B) \oplus B \quad (2)$$

$$\text{Closing: } A \bullet B = (A \oplus B) \square B \quad (3)$$

Where  $\square$  is the mathematical erosion operator and  $\oplus$  is the dilation operator. A is an image and B is a disc.

Morphological opening generally smooths the contour of an image, breaks narrow isthmuses, and eliminates thin protrusions. By applying this opening operation to the CSF region mask, most of the subarachnoid spaces were removed, as shown in Fig. 7(b). In this study, we used a 7x7 rectangular mask for the opening operation.

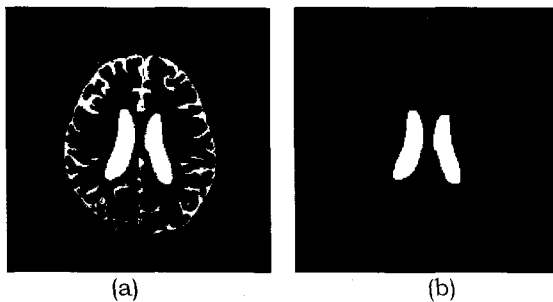


**Fig. 7.** Detection of lateral ventricle. (a) Segmented CSF region mask, (b) lateral ventricle detected using mathematical morphology opening operation.

After the detection of the ventricle, two morphological features were used to segment the periventricular WMC. First, the periventricular WMC can be clustered into the GM in the previous tissue segmentation process, even if they are included in the

white matter, because their intensity level is similar to that of the GM. This is not only the limitation of the intensity-based clustering method, but also the important motive in our method of detecting the periventricular WMC. Second, the periventricular WMC are distributed adjacent to the ventricle of the CSF. Finally, the ventricle is surrounded by white matter. Therefore, it is possible to segment the periventricular WMC by using these morphological features.

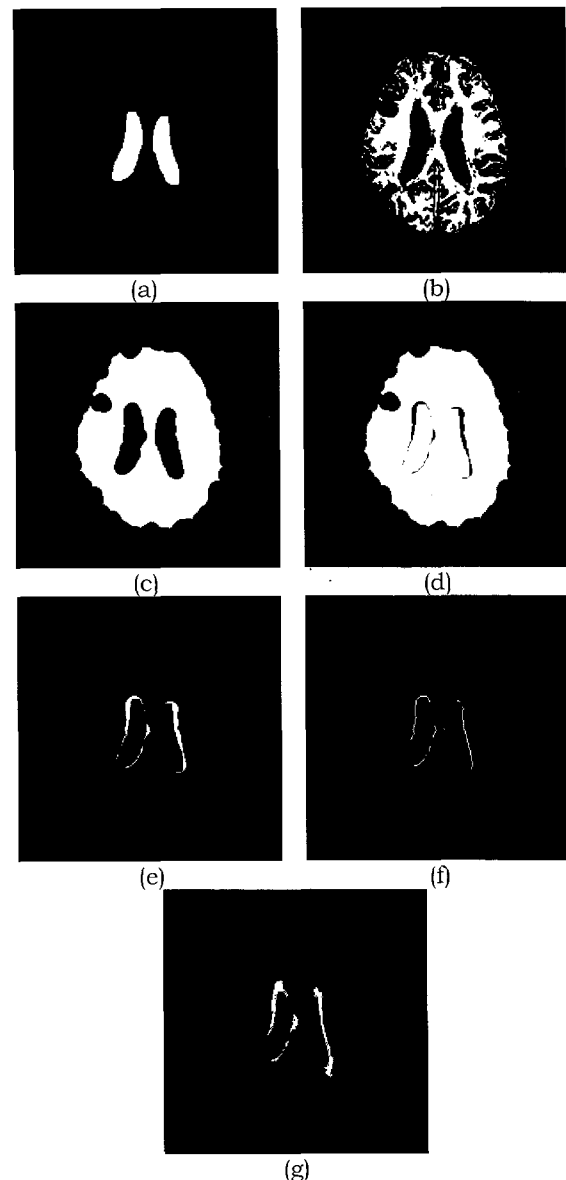


**Fig. 8.** Segmentation of periventricular WMC. (a) Segmented lateral ventricle, (b) WM region, (c) simplified image using morphological closing operation to segmented WM region mask, (d) overlapped image of segmented lateral ventricle and WM region, (e) candidate region between segmented lateral ventricle and WM region, (f) thinned image of candidate region and (g) final periventricular WMC.

To find the candidate region of the periventricular, the segmented ventricle image and segmented WM mask image were used. Firstly, to fill up any unnecessary holes in the subarachnoid space, a morphology closing operation, such as defined in Eq. (3), is applied to the segmented WM region mask (Fig. 8(c)). When the lateral ventricle and closed WM masks are merged, the blank space between the two masks may be considered as a candidate region for the periventricular WMC. This blank space can be obtained by using a morphology closing operation with a small size operating disc in the segmented lateral ventricle mask. To segment the periventricular WMC more accurately, we used the multi-seed region growing method. Although we may simply use the candidate region as seed points, it is preferable to make the initial candidate region thin, in order to reduce the number of initial seed points and computation time. Fig. 8(f) shows the thinned image of the candidate region, which is used as the initial seed points for the region growing method, and Fig. 8(g) shows the periventricular WMC segmented using the region growing method.

## RESULTS

The proposed method consists of several sub-processes. However for multiple sequential steps, no user interaction is needed except input file loading of T2 and PD images. In this section experiment results are described.

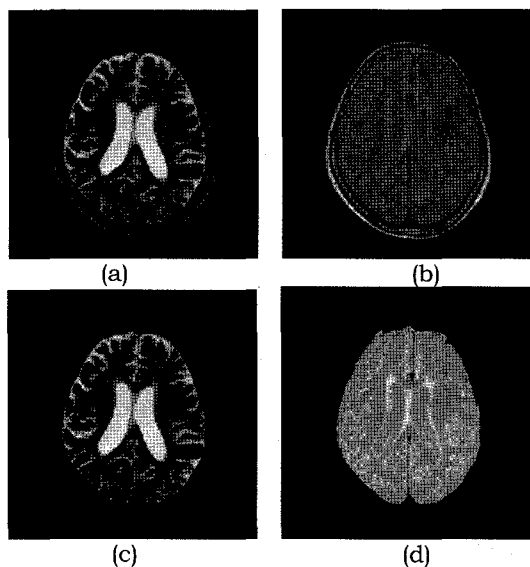


**Fig. 9.** Automatic skull and scalp stripping result of T2- and PD-weighted images. (a) T2-weighted image, (b) PD-weighted image, (c) stripped image of (a), (d) stripped image of (b).

In Fig. 9(c) and (d), most of the non-brain regions are removed by the proposed skull and scalp stripping algorithm. Although a small region remained, it did not affect the subsequent tissue segmentation operation and WMC detection result. In Fig. 8, the total computation time required for removing the skull from the T2- and PD-weighted images is 4.68 sec. In Fig. 10, (a), (b) and (c) show the brain tissue segmentation results obtained from the image stripped from skull and scalp (Fig. 9(c) and (d)). Fig. 9(a) shows the CSF region mask and Fig. 10(b) and (c) show the GM and WM region masks. In Fig. 10(b), a part of the white matter adjacent to the lateral ventricle is clustered as gray matter. To get resultant periventricular WMC, some sub processes are needed. In this study, the region growing method is also applied to the segmented GM image, in order to segment the periventricular WMC. The seed points used for region growing are set close to the boundary of the ventricle, because most of the periventricular WMC are adjacent to the lateral ventricle. Some points on the boundary could be used, because of the possibility that some of them do not correspond to the periventricular WMC. If it is applied to the boundary points which are out of the periventricular WMC range, the region growing method may result in incorrect segmentation. Therefore, the candidate region of the periventricular WMC must be correctly set for accurate segmentation to be obtained. Fig. 10(d) and (e) show the detection results of the overlapping WMC on the original T2- and PD-weighted images. The computation time required for the segmentation of the brain tissues and the detection of the periventricular WMC are about 5.36 sec and 2.46 sec, respectively. The total computation time required for the automatic detection of the periventricular WMC is 12.53 sec. and Table 1 shows final detection results for other patients.

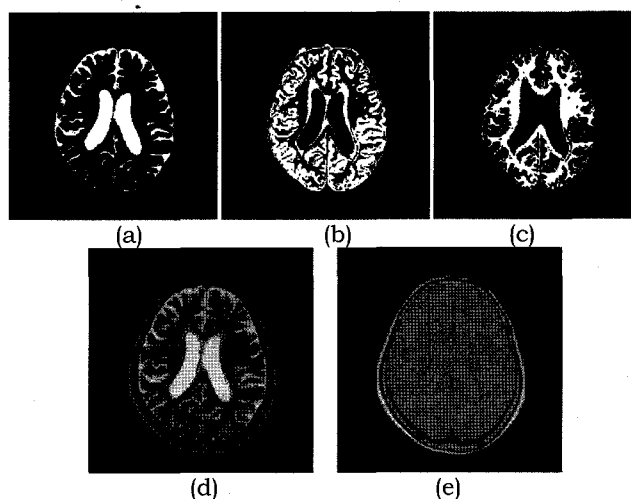


**Fig. 10.** Brain tissue segmentation and WMC detection. (a), (b) and (c) are the segmentation results of the brain tissue, including the CSF, GM and WM. The blue lined regions of (d) and (e) are the periventricular WMC detected by the proposed method.

## CONCLUSION AND DISCUSSION

In this paper, we proposed a fully automatic algorithm for the detection of periventricular WMC. Our algorithm consists of 3 steps as following skull and scalp stripping, the segmentation of the brain tissue including the CSF, GM and WM and, finally, the detection of the periventricular WMC.

As the first step of our overall algorithm, the skull and scalp stripping process, which removes non-brain regions from the PD-weighted image, makes use of the multi-seed region growing method. The PD-weighted image has less contrast than the T2-weighted image and, therefore, it is possible to obtain the intracranial mask using the multi-seed region growing method. Also, four seed points were selected from our brain model, by considering the shapes in both the cerebrum and cerebellum (Fig. 2). Our proposed stripping algorithm was able to successfully remove the non-brain regions in both the T2- and PD-weighted images in 5 sec.

Our segmentation algorithm used both the ratio image of the PD-weighted image to the T2-weighted image and the K-means clustering method sequentially. The former was used to segment the CSF region, while the latter was used to segment the GM and WM in the genuine brain images extracted from non-necessary skull and scalp. This segmentation step may affect the subsequent WMC detection step, because the WMC detection method was based on the results obtained during the segmentation step. The use of the ratio image of the PD- to the T2-weighted image [18], [19] allowed the CSF to be segmented faster than with any of the previous methods, such as the intensity-based classification technique, due to the combined use of the Otsu thresholding scheme [15]. The K-means clustering scheme, which is used to segment the GM and WM has an advantage in that it is simple and fast.

The last step is the detection of the periventricular WMC from the segmented results. To segment the periventricular WMC efficiently, we used its morphological features, in that they are located adjacent to the lateral ventricle. We separated the lateral ventricle from the segmented CSF region prior to the detection process. The final detection process used mathematical morphology operations and region growing methods.

The proposed algorithm uses the morphological features of the periventricular WMC, in the sense that they have an intensity level similar to that of the GM and are located adjacent to the lateral ventricle. From the segmentation results, it can be concluded that our assumptions are correct and that the proposed algorithm is very efficient at detecting and segmenting the periventricular WMC. Recently many brain image analysis systems support brain tissue extraction such as Brainsuite [22] and LONI pipeline processing system [23]. These tools offer many powerful segmentation algorithm and software modules, but usually their target application is a general brain tissue extraction

system so that it is not easy to use for specific application. Since methods used in above tools are mainly based on statistical algorithm with brain structure model. Hence for our target application, the proposed method may be more proper because it considers specific feature of periventricular WMC.

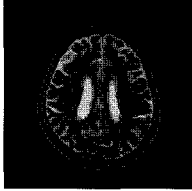
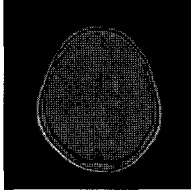
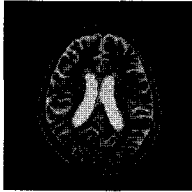
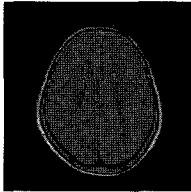
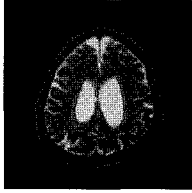
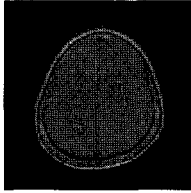
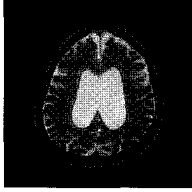
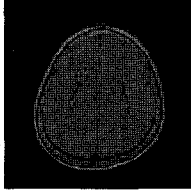
However, the proposed method has some limitations and problems. Firstly, the computation time needs to be reduced, even if the operation is performed fully automatically. In the experiment results, the proposed method needed between 10 sec and 15 sec to perform the processing required for the individual image slice set of T2- and PD-weighted images. Because the brain model for the detection of the seed points is made by considering the shapes of both the cerebrum and cerebellum, the proposed method selects four seed points. However, it is unnecessary to use all 4 seed points in the detection of the periventricular WMC, which are located in the lateral ventricle. Therefore, the computation time can be reduced, by using only two seed points and we confirmed this in a supplementary experiment. Table 1 shows the experiment results as a function of the number of seed points used. In several cases, we confirmed that the computation time was decreased by reducing the number of seed points, without there being any impact on the segmentation performance.

Actually, the K-means clustering process used for tissue segmentation was the most time consuming process, because the IDL language used in this implementation generally requires a long time to perform the loop operations, which are used repeatedly in K-means clustering. Therefore, this time could be reduced by implementing the program using a different language, such as C or C++.

One of the major limitations of the proposed algorithm is that the detection performance is dependent on the segmentation of the brain tissue. Poor segmentation induces inaccurate subsequent detection of the WMC and incorrect quantification results, because the morphological features of the periventricular WMC cannot be used efficiently in such cases.

Intensity-based clustering segmentation methods, such as the K-means clustering technique used in this study, depend on the changes in the intensity distribution of the images. One of the most critical problems which reduce the performance of intensity-based clustering methods in MR images is intensity non-uniformity [17], which is known to be induced by the inhomogeneous sensitivity profile of the surface-coil. When this happens, the same tissues may have different intensity levels and, therefore, successful segmentation using intensity-based clustering methods is difficult to accomplish. The K-means clustering method used in this paper also shows weak performance under conditions of intensity non-uniformity. To obtain high performance in spite of this intensity non-uniformity, it will be necessary to apply an intensity bias correction process prior to the segmentation process [17], [24].

**Table 1.** Computation time (sec) as a function of the number of seed points used in the skull and scalp stripping process. (62 (case 1 and 2) and 77 (case 3 and 4) years old woman with Alzheimer's disease)

	T2-weighted image	PD-weighted image	4 seed points (sec)	2 seed points (sec)
Case 1			11.32	10.14
Case 2			12.52	11.98
Case 3			12.80	11.24
Case 4			14.78	13.32

Finally, the proposed algorithm has not yet been validated statistically, by comparing its results with those obtained manually by experts. Although the proposed method shows qualitatively good results, quantitative analysis is needed for the verification of its accuracy and reproducibility. The detection of sub-cortical WMC and the statistical validation of this method against a gold standard remain as future works.

As MRI technology grows up new imaging techniques are developed. New types of images offer good quality for better diagnosis so many conventional diseases can be detected easily. In quantitative research using MRI, new imaging technique is also very helpful to users. In this paper, we used T2 and PD images together since PD has high contrast between GM and WM and CSF can be well identified in T2 image. If new imaging technique such as gradient-echo based T1 weighted image (T1WI) is used, we may get better result. However to obtain MRI data from real patients is still troublesome because of need for a lot of money and time. In generally, T2 and PD are very

usual sequence and even both of them can be scanned with one sequence. Therefore the proposed method is very economical in real application so that users and researchers without new imaging facility can also use it.

In conclusion, the proposed algorithm for the detection of periventricular WMC demonstrated its capacity to overcome the limitations of the previous intensity-based clustering method, based on the use of morphological features. Moreover, because the proposed algorithm is fully automatic, it can process a large amount of image data rapidly and efficiently. The proposed algorithm in conjunction with an intensity non-uniformity correction process has the potential to provide a powerful method of detecting periventricular WMC.

## REFERENCES

- [1] P. Sullivan, R. Pary, F. Telang, "Risk factors for white matter changes detected by magnetic resonance imaging



- in the elderly", *Stroke*, Vol. 21 pp. 1424–1428, 1990.
- [2] J. V. Swieten, S. Staal, L. Kappelle, M. Derix and J. V. Gijn, "Are white matter lesions directly associated with cognitive impairment in patients with lacunar infarcts?", *J. Neurol.*, Vol. 243, No. 2, pp.196–200, 1996.
- [3] C. DeCarli, B. Miller, G. Swan, T. Reed, P. Wolf and D. Carmelli, "Cerebrovascular and Brain Morphologic Correlates of Mild Cognitive Impairment in the National Heart, Lung, and Blood Institute Twin Study", *Arch. Neurol.*, Vol. 58, pp. 643–647, 2001.
- [4] S. Gupta, M. Naheedy, J. Young, M. Ghobrial, F. Rubino, W. Hindo, "Periventricular white matter changes and dementia. Clinical, neuropsychological, radiological, and pathological correlation", *Arch Neurol.*, Vol.45, pp. 637–641, 1988.
- [5] D. Snowdon, S. Kemper, J. Mortimer, L. Greiner, D. Wekstein and W. Markesbery, "Linguistic ability in early life and cognitive function and Alzheimer's disease in late life: Findings from the Nun Study", *Journal of the American Medical Association*, Vol. 275, pp. 528–532, 1996.
- [6] H. Wolf, G. Ecke, S. Bettin, J. Dietrich and H. Gertz, "Do white matter changes contribute to the subsequent development of dementia in patients with mild cognitive impairment? A longitudinal study", *International Journal of Geriatric Psychiatry*, Vol. 15, pp. 803–812, 2000.
- [7] L. Truyen, J. V. Waesberghe, M. V. Walderveen, B. V. Oosten, C. Polman, O. Hommes, H. Ader and F. Barkhof, "Accumulation of hypointense lesions ("black holes") on T1 spin-echo MRI correlates with disease progression in multiple sclerosis", *Neurology*, Vol. 47, pp. 1469–1476, 1996.
- [8] M. V. Walderveen, F. Barkhof, H. ommes, C. Polman, H. Tobi, S. Frequin and J. Valk, "Correlating MRI and clinical disease activity in multiple sclerosis: relevance of hypointense lesions on short-TR/short-TE (T1-weighted) spin-echo images", *Neurology*, Vol. 45, pp. 1684–1690, 1995.
- [9] F. Pannizzo, M.J.B. Stallmeyer, J. Friedman, R.J. Jennis, J. Zabriskie, C. Pland, R. Zimmerman, J.P. Whalen, and P.T. Cahill, "Quantitative MRI studies for assessment of multiple sclerosis", *Magnetic Resonance in Medicine*, Vol. 24 pp. 90–99, 1992.
- [10] S. Warfield, "Fast k-NN classification for multichannel image data", *Pattern Recog. Lett.*, Vol. 17 No. 7, pp. 713–721, 1996.
- [11] N. A. Mohamed, M. N. Ahmed and A. A. Farag, "Modified fuzzy C-mean in medical image segmentation", *Proc. IEEE International Conference on Acoustics, Speech, and Signal Processing (ICASSP'99)*, Vol. 6, pp. 3429 - 3432, March 1999.
- [12] S. Z. Selim and M. A. Ismail, "K-means-type algorithms", *IEEE Trans. Pattern Anal. Machine Intell.*, Vol. 6, pp. 81–87, Jan. 1984.
- [13] E. Ardizzone, R. Pirrone, O. Gambino and D. Peri, "Two channels fuzzy c-means detection of multiple sclerosis lesions in multispectral MR images", *Image Processing., International Conference on*, Vol.2, pp. 345–348, 2002.
- [14] M. Joshi, J. Cui, K. Doolittle, S. Joshi, D. V. Essen, L. Wang and Michael I. Miller, "Brain Segmentation and the Generation of Cortical Surfaces", *NeuroImage*, Vol. 9, Iss. 5, pp. 461–476, May 1999.
- [15] N. Otsu, "A threshold selection method from gray-level histogram", *IEEE Transactions on System, Man, and Cybernetics*, SMC-8, pp. 62–66, 1978.
- [16] R. Adams and L. Bischof, "Seeded region growing", *IEEE Trans. Pattern Anal. Machine Intell.*, Vol. 16, pp. 641–647, 1994.
- [17] M. Styner, C. Brechbuhler, G. Szckely and G. Gerig, "Parametric estimate of intensity inhomogeneities applied to MRI", *IEEE Transactions on Medical Imaging*, Vol. 19, Issue. 3, Mar 2000, pp. 153–165.
- [18] M. G. Ballester, A. P. Zisserman and M. Brady, "Estimation of the partial volume effect in MRF", *Medical Image Analysis*, Vol. 6, Iss. 4, pp. 389–405, Dec. 2002.
- [19] W. K. Pratt, Chapter 12.9. Multispectral Image Enhancement, *Digital Image Processing*, New York: Wiley, 1978.
- [20] H. S-Zadeh, J. P. Windham, D. J. Peck and A. E. Yagle, "A Comparative Analysis of Several Transformations for Enhancement and Segmentation of Magnetic Resonance Image Scene Sequences", *IEEE Transactions on Medical Imaging*, Vol. 11, No. 3, pp. 302–318, 1992.
- [21] R. C. Gonzalez and R. E. Woods, *Digital Image Processing*, Addison-Wesley Publishing Company, Inc., 1992.
- [22] D. W. Shattuck and R. M. Leahy, "BrainSuite: An automated cortical surface identification tool", *Medical Image Analysis*, Vol. 6, Iss. 2, pp. 129–142, June 2002.
- [23] D. E. Rex, J Q. Ma and A. W. Toga, "The LONI Pipeline Processing Environment", *NeuroImage*, Vol. 19, Iss. 3, pp. 1033–1048, July 2003.
- [24] J. Sled, A. Zijdenbos, A. Evans, "A nonparametric method for automatic correction of intensity nonuniformity in MRI data", *IEEE Transactions on Medical Imaging*, Vol. 7, Issue. 1, pp. 87 – 97, Feb. 1998.